HHS Public Access

Author manuscript

Int J Radiat Oncol Biol Phys. Author manuscript; available in PMC 2016 June 01.

Published in final edited form as:

Int J Radiat Oncol Biol Phys. 2015 June 1; 92(2): 430–437. doi:10.1016/j.ijrobp.2015.01.035.

High quality T2-weighted 4D magnetic resonance imaging for radiation therapy applications

Dongsu Du, MS[1], **Shelton D. Caruthers, PhD**[2], **Carri Glide-Hurst, PhD**[3], **Daniel A. Low, PhD**[4], **H. Harold Li, PhD**[1], **Sasa Mutic, PhD**[1], and **Yanle Hu, PhD**[1,5]

[1]Department of Radiation Oncology, Washington University School of Medicine, Saint Louis, MO, USA

[2]Philips Healthcare, Cleveland, OH, USA

[3]Department of Radiation Oncology, Henry Ford Health System, Detroit, MI, USA

[4]Department of Radiation Oncology, University of California Los Angeles, Los Angeles, CA, USA

[5]Department of Radiation Oncology, Mayo Clinic in Arizona, Phoenix, AZ, USA

Abstract

Purpose—To improve triggering efficiency of the prospective respiratory amplitude triggered 4DMRI method and to develop a 4DMRI imaging protocol that can offer T2 weighting for better tumor visualization, good spatial coverage, spatial resolution and respiratory motion sampling within a reasonable amount of time for radiation therapy applications.

Methods and Materials—The respiratory state splitting (RSS) method and the multi-shot acquisition (MSA) method were analytically compared and validated in a simulation study using the respiratory signals from 10 healthy human subjects. The RSS method was identified to be more effective in improving triggering efficiency. It was implemented in the prospective respiratory amplitude triggered 4DMRI. 4DMRI image datasets were acquired from 5 healthy human subjects. Liver motion was estimated using the acquired 4DMRI image datasets.

Results—The simulation study showed that the RSS method was more effective in improving triggering efficiency compared to the MSA method. The average reductions in 4DMRI acquisition time were 36% and 10% for the RSS and MSA methods, respectively. The human subject study showed that T2-weighted 4DMRI with 10 respiratory states, 60 slices at a spatial resolution of $1.5\times1.5\times3.0$ mm^3 could be acquired in 9-18 minutes, depending on individual's breath pattern. Based on the acquired 4DMRI image datasets, the ranges of peak-to-peak liver displacements among 5 human subjects were 9.0-12.9 mm, 2.5-3.9 mm and 0.5-2.3 mm in superior-inferior, anterior-posterior and left-right directions, respectively.

Correspondence should be directed to: Yanle Hu, Ph.D. Department of Radiation Oncology, Mayo Clinic in Arizona, 5777 E Mayo Blvd, Phoenix, AZ 85054, USA, Tel: 480-342-2922, Hu.Yanle@mayo.edu.

Conflict of interest: Dr. Caruthers is an employee of Phillips Healthcare.

Conclusions—We demonstrated that with the RSS method, it was feasible to acquire high quality T2-weighted 4DMRI within a reasonable amount of time for radiation therapy applications.

Keywords

T2 weighted 4DMRI; Amplitude triggered; High spatial and temporal resolution

Introduction

Respiration-induced organ and tumor motion imposes significant challenges in the radiation therapy treatment of abdominal and lung cancers. Studies have shown that peak-to-peak tumor or organ motion can be as large as 2-3 cm (1-5). To ensure sufficient dose coverage to the target, a large treatment margin has to be used (6-9), which unavoidably increases radiation dose to radiosensitive critical structures surrounding the target, causing increased side effects. Reducing the treatment margin without sacrificing dose coverage requires effective motion management, for which accurate knowledge of respiration induced motion is essential.

Four-dimensional computed tomography (4DCT) (10-13) is commonly used to provide respiration-induced motion information. However, for abdominal cancer where the tumor is embedded in the soft tissue, the low tumor tissue contrast of CT images makes 4DCT less useful and therefore limits its applications. To improve soft tissue and tumor tissue contrast, 4D Magnetic Resonance Imaging (4DMRI) has been developed using either retrospective sorting (14-19) or prospective triggering (20, 21) techniques. 4DMRI (T2-weighted) is able to provide accurate tumor motion information, from which internal target volume can be derived for the subsequent treatment planning in a way similar to what 4DCT does but more powerful for abdominal cancers. In addition, tumor motion information is useful in 4D radiation therapy (22), e.g. gated dose delivery.

Compared to retrospective 4DMRI, prospective 4DMRI acquires images during specific respiratory states that meet predefined criteria, resulting in improved acquisition efficacy, reduced acquisition time and increased robustness to breathing irregularity. More importantly, with am amplitude based prospective triggering system, images of a single slice at different respiratory states no longer have to be acquired consecutively within one respiratory cycle. They can be separated into multiple respiratory cycles to allow complete relaxation of magnetization. This overcomes the upper limit placed on repetition time (TR) and therefore can accommodate more MRI sequences including those with better tumor tissue contrast such as T2-weighted MRI (20), allowing motion tracking of the tumor itself. In a feasibility study, Hu *et al* (20) reported that under prospective guidance based on respiratory amplitude, T2 weighted 4DMRI with 32 slices, 4 states per respiratory cycle and $1.5\times1.5\times5.0$ mm^3 spatial resolution could be obtained within a few minutes. However, more respiratory states and slices are typically required for radiation therapy applications.

As numbers of slices and respiratory states increase, 4DMRI image acquisition time increases substantially. While increasing the number of slices prolongs the 4DMRI acquisition time linearly, increasing the number of respiratory states has more dramatic,

non-linear effect on the 4DMRI acquisition time, primarily due to frequent trigger missing. Here, trigger missing indicates a situation in which the respiratory amplitude that triggers image acquisition of a particular slice appears before the image acquisition completion of the previous slice and therefore gets ignored by the MRI scanner. As the number of respiratory states increases, the number of slices that needs to be acquired in a respiratory cycle increases (cf. Figure 1a & b). Accordingly, the amount of time allocated for the image acquisition of each slice decreases. When the allocated time becomes less than the required image acquisition time of a slice, overlaps in image acquisition can happen, thereby causing trigger missing events, especially at mid inhalation and mid exhalation as shown in Figure 1 a & b. Frequent trigger missing can reduce triggering efficiency tremendously, thereby increasing the 4DMRI acquisition time because the MRI scanner has to pause and wait for the same respiratory amplitude to appear again, which is at least one respiratory cycle later.

The purpose of this study is to 1) investigate methods to improve triggering efficiency of the prospective respiratory amplitude triggered 4DMRI by mitigating the trigger missing issue associated with increased number of respiratory states, and 2) develop an imaging protocol to acquire T2 weighted 4DMRI within a reasonable amount of acquisition time to offer good spatial coverage and resolution, and sufficient respiratory motion sampling. Both simulations and experiments on healthy human subjects were performed in this study.

Methods and Materials

Human subjects

10 healthy adult human subjects, including both female and male, were enrolled in this study to validate the methodology. The respiratory signals from 5 human subjects were acquired for the simulation purpose only. Both the respiratory signal and 4DMRI image dataset were acquired for the rest 5 human subjects. This study was approved by the Institutional IRB office.

Potential solutions

To mitigate the trigger missing issue due to the increased number of respiratory states, we could either increase the amount of time allocated for the image acquisition of a single slice (Figure 1c), or decrease the image acquisition time of each respiratory state (Figure 1d). Splitting all respiratory states into multiple groups in an interleaved manner and acquiring each group of respiratory states independently increases the amount of time available for image acquisition of a slice by a factor of the number of groups. This method is referred to as the respiratory state splitting (RSS) method. Although the nominal 4DMRI acquisition time also increases by a factor of the number of groups, the RSS method can effectively reduce the chance of trigger missing, thereby reducing the total 4DMRI acquisition time. Dividing the required k-space data for a single slice into multiple segments and acquiring one segment of k-space data at a time following each respiratory trigger can decrease the image acquisition time at each respiratory state by a factor of the number of segments and therefore mitigate the trigger missing issue. This method is referred to as the multi-shot acquisition (MSA) method.

Analytical comparison

An analytical comparison was performed to compare the efficiencies of the RSS and MSA methods in reducing 4DMRI image acquisition time. Assume that the number of slices is N_{Slice}, the number of respiratory states is N_{RS}, the number of groups in the RSS method is N_{Group}, the number of shots in the MSA method is N_{Shot}, the average respiratory period is T_{Resp}, the single shot acquisition time for a 2D slice is T_{SSAcq} and the time between two consecutive shot acquisitions (or triggers) is t_{AcqInt},_the total 4DMRI acquisition time for the RSS method (T_{RSS}) and the MSA method (T_{MSA}) can be estimated using Equations (1) and (2), respectively.

$$T_{RSS}=T_{Resp}\cdot\frac{N_{Slice}}{N_{RS}/N_{Group}}\cdot N_{RS}+T_{Resp}\cdot\sum_{m=1}^{N_{Slice}}\sum_{n=1}^{N_{RS}}P(t_{AcqInt}<T_{SSAcq}) \quad (1)$$

$$T_{MSA}=T_{Resp}\cdot\frac{N_{Slice}}{N_{RS}}\cdot N_{RS}\cdot N_{Shot}+T_{Resp}\cdot\sum_{m=1}^{N_{Slice}}\sum_{n=1}^{N_{RS}}\left(\sum_{l=1}^{N_{Shot}}P(t_{AcqInt,l}<\frac{T_{SSAcq}}{N_{Shot}})\right) \quad (2)$$

Here $P(\cdot)$ indicates the chance of trigger missing. If the formula inside the parentheses is true, then $P(\cdot) = 1$, indicating a trigger missing event. Otherwise, $P(\cdot) = 0$, indicating no trigger missing. In the equations (1) and (2), the first term represents the 4DMRI acquisition time without considering the trigger missing issue and the second term indicates the added acquisition time caused by the missing triggers.

For a direct comparison, we assume that $N_{Group} = N_{Shot}$. Therefore, the first term in the two equations becomes identical. The second term differs in the way to calculate the chance of trigger missing, which is $P(t_{AcqInt} < T_{SSAcq})$ for the RSS method and $\sum_{l=1}^{N_{Shot}}P(t_{AcqInt,l}<\frac{T_{SSAcq}}{N_{Shot}})$ for the MSA method. Mathematically, the following inequality is always true.

$$P(t_{AcqInt}<T_{SSAcq})\leq\sum_{l=1}^{N_{Shot}}P(t_{AcqInt,l}<\frac{T_{SSAcq}}{N_{Shot}}) \quad (3)$$

Proof: From the trigger missing point of view and assume $N_{Group} = N_{Shot}$, t_{AcqInt} in the RSS method shall equal $\sum_{l=1}^{N_{Shot}}t_{AcqInt,l}$ in the MSA method. Since the goal is to estimate the probability of trigger missing, for the moment we can neglect the requirement for MRI contrast formation, *e.g*. multiple shots for the same slice cannot be acquired consecutively.

When $t_{AcqInt} > T_{SSAcq}$ and $t_{AcqInt,l}>\frac{T_{SSAcq}}{N_{Shot}}$, *for* $l = 1,\ldots, N_{Shot}$, then $P(\cdot) = 0$ for both methods.

Therefore, the above inequality (3) holds true. Due to the fact that $t_{AcqInt,l}>\frac{T_{SSAcq}}{N_{Shot}}, for\, l=1,\cdots,N_{Shot}\Rightarrow\sum_{l=1}^{N_{Shot}}t_{AcqInt,l}>T_{SSAcq}\Rightarrow t_{AcqInt}>T_{SSAcq}$, when t_{AcqInt}

$< T_{SSAcq}$, then $t_{AcqInt,l} < \frac{T_{SSAcq}}{N_{Shot}}$ holds true for at least one shot out of N_{Shot} in the MSA method. In such a situation, $P(t_{AcqInt} < T_{SSAcq}) = 1$ for the RSS method and $\sum_{l=1}^{N_{Shot}} P(t_{AcqInt,l} < \frac{T_{SSAcq}}{N_{Shot}}) \geq 1$ for the MSA method. Therefore, the above inequality (3) holds true as well.

Based on Equation (1) and (2), as well as Inequality (3), we can reach the conclusion that T_{RSS} is always equal or less than T_{MSA}. The analytical comparison is in favor of the RSS method.

Simulation study

A simulation study was performed using MATLAB (The MathWorks Inc., Natick, MA) to evaluate the performance of the RSS and MSA methods in reducing 4DMRI acquisition time. Respiratory signals were acquired from 10 healthy human subjects (5 prospective and 5 retrospective) using a standard air cushion bellow wrapped around subjects' abdomen. Three triggering strategies (no intervention, RSS and MSA) were applied to the respiratory signals to simulate 4DMRI acquisition times. The 4DMRI acquisition time using the original prospective 4DMRI with no intervention applied to address the trigger missing issue was used as the reference to calculate the percentage reduction in the acquisition time for 4DMRI using the RSS and MSA methods. The parameters used in the simulation study were $N_{Slice} = 60$, $N_{RS} = 10$, $N_{Group} = N_{shot} = 2$ and $T_{SSAcq} = 380$ *ms*. Respiratory trigger acceptance range was set to be 5% of the respiratory range placed at each triggering respiratory amplitude (or respiratory state). The 5% window was determined empirically based on tradeoff between the expected liver displacement, scan efficiency, and triggering accuracy. When respiratory amplitude falls within the acceptance range, a trigger is sent to start image acquisition. In the simulation study, image acquisition time (either T_{SSAcq} or T_{SSAcq}/N_{Shot}) was placed after each respiratory trigger to simulate the image acquisition and no real MRI data acquisition was actually involved. Results of the simulation study are listed in the RESULTS section, which support the superiority of the RSS method.

Human subject study – 4DMRI acquisition

Since both the analytical comparison and the simulation study showed that the RSS method was more effective in reducing 4DMRI acquisition time, we chose this technique for the human subject study and implemented it into a respiratory amplitude triggered T2 weighted TSE (Turbo Spin Echo) 4DMRI sequence (20) using the Philips PARADISE pulse sequence programming environment (Philips Healthcare, Andover, MA, version R2.5.3).

Five healthy human subjects were scanned on a Philips Achieva 1.5T MRI scanner (Philips Healthcare, Andover, MA). The integrated body coil was used as the transmitter and the 4-channel receive-only phase array coil was used as the receiver. An air-filled cushion with a pressure sensor was placed on the abdomen of the human subject and secured by a belt wrapped around the human subject to provide the respiratory signal that triggered the 4DMRI image acquisition. Since respiratory-induced organ motion is mainly in the superior-inferior direction, 4DMRI images were acquired in the sagittal orientation around the

abdominal area. Sixty 3 mm slices with no gap were acquired to provide 180 mm coverage in the lateral direction. The in-plane field of view (FOV) was 375 × 260 mm^2 and the in-plane spatial resolution was 1.5 × 1.5 mm^2. Single-shot spin echo was used to acquire each 2D image. Parallel imaging with an accelerator factor of 2 and partial-k acquisition with 70% k-space coverage were utilized to reduce the acquisition time for each 2D image (T_{SSAcq}) to 380 ms. Within the 380 ms, the first 250 ms was devoted to image acquisition which determined image quality and the next 130 ms was merely waiting time to satisfy the specific absorption rate (SAR) requirement. Ten respiratory states were acquired. They were evenly separated into two groups in an interleaved manner (Figure 1c). The nominal scan time without respiratory triggering was 3 minutes 42 seconds. The acquired 2D images were arranged into 3D volumes based on respiratory states. 3D volumes at 10 respiratory states were assembled together to form a complete 4DMRI image dataset, which was subsequently used to estimate liver motion.

Liver motion estimation

Liver motion was characterized using deformation vector field (DVF) analysis in a manner similar to that reported in previous studies (18, 23). Note that other techniques to measure liver motion have been reported such as template tracking (24) and centroid displacement (25). Because images were acquired on healthy volunteers and no tumors were involved, DVF analysis was appropriate to provide motion information of the entire liver. A non-rigid image registration was applied between the 3D volumetric images at a given respiratory state and those at the end-of-exhalation using an open source MIRT (medical imaging registration tool) software (26). This software utilizes B-spline based non-rigid registration (27). The deformation between the two volumes was represented by a 3D vector matrix, indicating the motion of each voxel relative to its 3D location at the end of exhalation. Because this was a single modality image registration, we employed SSD (Sum of squared differences) as the similarity measurement. The maximum liver motions were calculated using the DVF.

Results

Simulation study

The simulated acquisition times for 4DMRI methods incorporating no intervention, RSS and MSA were listed in Table 1. The average reductions in acquisition time were 36% and 10% for the RSS and the MSA methods, respectively. Figure 2 shows the simulated 4DMRI acquisition from a representative human subject for each of the three methods. The RSS method was more time efficient compared to the other two methods.

Human subject study

Using the RSS method, the 4DMRI acquisition times were 9.9, 16.1, 17.8, 13.1 and 8.9 minutes for the 5 healthy human subjects (subject #6 to subject #10 in Table 1), which were within half a minute of the simulated acquisition times. Figure 3 shows images of a representative sagittal slice at the 10 respiratory states (0%, 20%↑, 40%↑, 60%↑, 80%↑, 100%, 80%↓, 60%↓, 40%↓ and 20%↓ where ↑ indicates inhalation and ↓ indicates exhalation) for the 5 human subjects. With the aid of a white line placed on the liver dome at

the end of exhalation, the respiration-induced liver motion can be easily visualized. Note that breathing motion may manifest a hysteresis behavior in which lung tissue, as well as the diaphragm, moves in different paths during inhalation and exhalation (28, 29). It was hypothesized that this was caused by pressure imbalances within the lung tissue during breathing (30). The hysteresis motion behavior was observed in subject a (Figure 3a) in which diaphragm motion is relatively linear during inhalation but quite non-linear during exhalation. Figure 4 shows the reconstructed images of a representative coronal plane at the 10 respiratory states for the 5 human subjects. The boundaries of the liver and kidney are smooth, indicating that images in each 3D volume were indeed acquired at the same respiratory state.

Liver motion estimation

Figure 5 shows the deformation vectors in the liver on top of the end-of-exhalation images in three orthogonal views. The deformation vectors were obtained from the deformable registration between the end-of-exhalation and end-of-inhalation volumetric images. The arrows started from the locations at the end-of-exhalation and pointed towards the locations at the end-of-inhalation. The liver motion was large in the superior-inferior (SI) direction, medium in the anterior-posterior (AP) direction and small in the left-right (LR) direction. The peak-to-peak liver displacements in SI, AP and LR directions were 11.2 mm, 3.2 mm, 0.8 mm for the subject #1, 10.7 mm, 2.8 mm, and 0.9 mm for the subject #2, 12.1 mm, 3.4 mm, and 0.5 mm for the subject #3, 9.0 mm, 3.9 mm, and 1.5 mm for the subject #4, 12.9 mm, 2.5 mm, and 2.3 mm for the subject #5, respectively.

Discussion

In this work, we have investigated methods (RSS and MSA) to mitigate the trigger missing issue in 4DMRI image acquisition that is often associated with the increased number of respiratory states. The RSS method was identified to be more effective and therefore implemented in the prospective respiratory amplitude triggered 4DMRI pulse sequence and validated using multiple healthy human subjects. It has been shown that with the RSS method, we were able to provide a practical 4DMRI protocol for radiation therapy applications, which offers T2 weighting for improved tumor tissue contrast, 10 respiratory states for sufficient respiratory motion sampling, 60 slices with 3 mm slice thickness for good spatial coverage, 1.5 mm in-plane spatial resolution for tumor delineation and a reasonable acquisition time between 9-18 minutes depending on the individual breathing pattern. We demonstrated that it was possible to estimate the liver motion using the acquired 4DMRI image datasets.

The RSS and MSA methods can reduce the chance of trigger missing and consequently the 4DMRI acquisition time. On the other hand, breaking the acquisition into multiple groups or shots will increase the total 4DMRI acquisition time by a factor of N_{Group}, or N_{Shot}. The net effect of the two competing factors determines the ultimate 4DMRI acquisition time. It is possible that the added scan time caused by using multiple groups (RSS) or shots (MSA) may exceed the reduced scan time resulting from less chance of trigger missing. Under such circumstance, the overall 4DMRI acquisition time may increase. This is observed for subject

#8 using the MSA method (Table 1). For the RSS method, the net effect was always a reduction in the 4DMRI acquisition time compared to the original prospective 4DMRI method incorporating no intervention.

In this study, DVF analysis was used to characterize liver motion. The accuracy of the DVF inside the liver, however, is difficult to evaluate due to the lack of contrast and feature, which is a limitation of the current study. In future patient studies, the good tumor tissue contrast of the T2-weighted images will provide a good visualization of the tumor (the most important ROI). The accuracy of the DVF can then be evaluated by comparing tumor motion obtained using the DVF and physician's manual contouring.

For human subjects, breathing patterns show irregularity in both amplitude and period (31, 32). For all respiratory signals used in this study, we didn't notice baseline drift over the long period of time (over 10 minutes). The respiratory baseline may experience drift in a relatively short time range but returns to previous level eventually. Therefore, it may be treated as one type of irregularity in amplitude. The prospective respiratory-amplitude-based 4DMRI acquires images only when pre-determined conditions are met. Therefore, it is less susceptible to breathing irregularity compared to retrospective 4DMRI, at a cost of lengthened acquisition time. The similar rationale has been applied to prospective acquisition for 4DCT (33). One limitation of prospective triggering approach is that if patient's breathing pattern/baseline changes substantially between the preparation and acquisition stages, the acquisition time will be prolonged. If long pauses are observed by the operator, the scan can be restarted to generate a new calibration based on the external surrogate.

Acknowledgments

This work is supported in part by National Institutes of Health grant 1R21CA167092

References

1. Gierga DP, Chen GT, Kung JH, et al. Quantification of respiration-induced abdominal tumor motion and its impact on IMRT dose distributions. Int J Radiat Oncol Biol Phys. 2004; 58:1584–1595. [PubMed: 15050340]
2. Langen KM, Jones DT. Organ motion and its management. Int J Radiat Oncol Biol Phys. 2001; 50:265–278. [PubMed: 11316572]
3. Suramo I, Paivansalo M, Myllyla V. Cranio-caudal movements of the liver, pancreas and kidneys in respiration. Acta Radiol Diagn (Stockh). 1984; 25:129–131. [PubMed: 6731017]
4. Bryan PJ, Custar S, Haaga JR, et al. Respiratory movement of the pancreas: an ultrasonic study. J Ultrasound Med. 1984; 3:317–320. [PubMed: 6748150]
5. Brock KK, Hollister SJ, Dawson LA, et al. Technical note: creating a four-dimensional model of the liver using finite element analysis. Med Phys. 2002; 29:1403–1405. [PubMed: 12148719]
6. Shirato H, Shimizu S, Kunieda T, et al. Physical aspects of a real-time tumor-tracking system for gated radiotherapy. Int J Radiat Oncol Biol Phys. 2000; 48:1187–1195. [PubMed: 11072178]
7. Hanley J, Debois MM, Mah D, et al. Deep inspiration breath-hold technique for lung tumors: the potential value of target immobilization and reduced lung density in dose escalation. Int J Radiat Oncol Biol Phys. 1999; 45:603–611. [PubMed: 10524412]
8. Rosenzweig KE, Hanley J, Mah D, et al. The deep inspiration breath-hold technique in the treatment of inoperable non-small-cell lung cancer. Int J Radiat Oncol Biol Phys. 2000; 48:81–87. [PubMed: 10924975]

9. Kubo HD, Hill BC. Respiration gated radiotherapy treatment: a technical study. Phys Med Biol. 1996; 41:83–91. [PubMed: 8685260]
10. Beddar AS, Kainz K, Briere TM, et al. Correlation between internal fiducial tumor motion and external marker motion for liver tumors imaged with 4D-CT. Int J Radiat Oncol Biol Phys. 2007; 67:630–638. [PubMed: 17236980]
11. Pan T, Lee TY, Rietzel E, et al. 4D-CT imaging of a volume influenced by respiratory motion on multi-slice CT. Med Phys. 2004; 31:333–340. [PubMed: 15000619]
12. Vedam SS, Keall PJ, Kini VR, et al. Acquiring a four-dimensional computed tomography dataset using an external respiratory signal. Phys Med Biol. 2003; 48:45–62. [PubMed: 12564500]
13. Keall PJ, Starkschall G, Shukla H, et al. Acquiring 4D thoracic CT scans using a multislice helical method. Phys Med Biol. 2004; 49:2053–2067. [PubMed: 15214541]
14. Cai J, Chang Z, Wang Z, et al. Four-dimensional magnetic resonance imaging (4D-MRI) using image-based respiratory surrogate: a feasibility study. Med Phys. 2011; 38:6384–6394. [PubMed: 22149822]
15. Tryggestad E, Flammang A, Han-Oh S, et al. Respiration-based sorting of dynamic MRI to derive representative 4D-MRI for radiotherapy planning. Med Phys. 2013; 40:051909. [PubMed: 23635279]
16. Tryggestad E, Flammang A, Hales R, et al. 4D tumor centroid tracking using orthogonal 2D dynamic MRI: implications for radiotherapy planning. Med Phys. 2013; 40:091712. [PubMed: 24007145]
17. Yang J, Cai J, Wang H, et al. Four-dimensional magnetic resonance imaging using axial body area as respiratory surrogate: initial patient results. Int J Radiat Oncol Biol Phys. 2014; 88:907–912. [PubMed: 24444759]
18. von Siebenthal M, Szekely G, Gamper U, et al. 4D MR imaging of respiratory organ motion and its variability. Phys Med Biol. 2007; 52:1547–1564. [PubMed: 17327648]
19. von Siebenthal M, Cattin P, Gamper U, et al. 4D MR imaging using internal respiratory gating. Med Image Comput Comput Assist Interv. 2005; 8:336–343. [PubMed: 16685977]
20. Hu Y, Caruthers SD, Low DA, et al. Respiratory amplitude guided 4-dimensional magnetic resonance imaging. Int J Radiat Oncol Biol Phys. 2013; 86:198–204. [PubMed: 23414769]
21. Tokuda J, Morikawa S, Haque HA, et al. Adaptive 4D MR imaging using navigator-based respiratory signal for MRI-guided therapy. Magn Reson Med. 2008; 59:1051–1061. [PubMed: 18429011]
22. Li G, Citrin D, Camphausen K, et al. Advances in 4D medical imaging and 4D radiation therapy. Technol Cancer Res Treat. 2008; 7:67–81. [PubMed: 18198927]
23. Williams CL, Mishra P, Seco J, et al. A mass-conserving 4D XCAT phantom for dose calculation and accumulation. Med Phys. 2013; 40:071728. [PubMed: 23822432]
24. Shi X, Diwanji T, Mooney KE, et al. Evaluation of template matching for tumor motion management with cine-MR images in lung cancer patients. Med Phys. 2014; 41:052304. [PubMed: 24784397]
25. Gauthier JF, Varfalvy N, Tremblay D, et al. Characterization of lung tumors motion baseline using cone-beam computed tomography. Med Phys. 2012; 39:7062–7070. [PubMed: 23127097]
26. Myronenko A, Song X. Intensity-based image registration by minimizing residual complexity. IEEE Trans Med Imaging. 2010; 29:1882–1891. [PubMed: 20562036]
27. Rueckert D, Sonoda LI, Hayes C, et al. Nonrigid registration using free-form deformations: application to breast MR images. IEEE Trans Med Imaging. 1999; 18:712–721. [PubMed: 10534053]
28. Seppenwoolde Y, Shirato H, Kitamura K, et al. Precise and real-time measurement of 3D tumor motion in lung due to breathing and heartbeat, measured during radiotherapy. Int J Radiat Oncol Biol Phys. 2002; 53:822–834. [PubMed: 12095547]
29. Boldea V, Sharp GC, Jiang SB, et al. 4D-CT lung motion estimation with deformable registration: quantification of motion nonlinearity and hysteresis. Med Phys. 2008; 35:1008–1018. [PubMed: 18404936]
30. Low DA, Parikh PJ, Lu W, et al. Novel breathing motion model for radiotherapy. Int J Radiat Oncol Biol Phys. 2005; 63:921–929. [PubMed: 16140468]

31. Glide-Hurst CK, Schwenker Smith M, Ajlouni M, et al. Evaluation of two synchronized external surrogates for 4D CT sorting. J Appl Clin Med Phys. 2013; 14:4301. [PubMed: 24257273]
32. Ruan D, Fessler JA, Balter JM, et al. Real-time profiling of respiratory motion: baseline drift, frequency variation and fundamental pattern change. Phys Med Biol. 2009; 54:4777–4792. [PubMed: 19622852]
33. Langner UW, Keall PJ. Prospective displacement and velocity-based cine 4D CT. Med Phys. 2008; 35:4501–4512. [PubMed: 18975697]

Summary

We investigated methods to improve triggering efficiency of the prospective respiratory amplitude triggered 4DMRI method, implemented the most effective one and validated it using a human study. The new 4DMRI method is able to provide T2 weighting with good spatial coverage, spatial resolution and respiratory motion sampling within a reasonable amount of time for radiation therapy applications. Liver motion was estimated using the acquired T2-weighted 4DMRI image datasets.

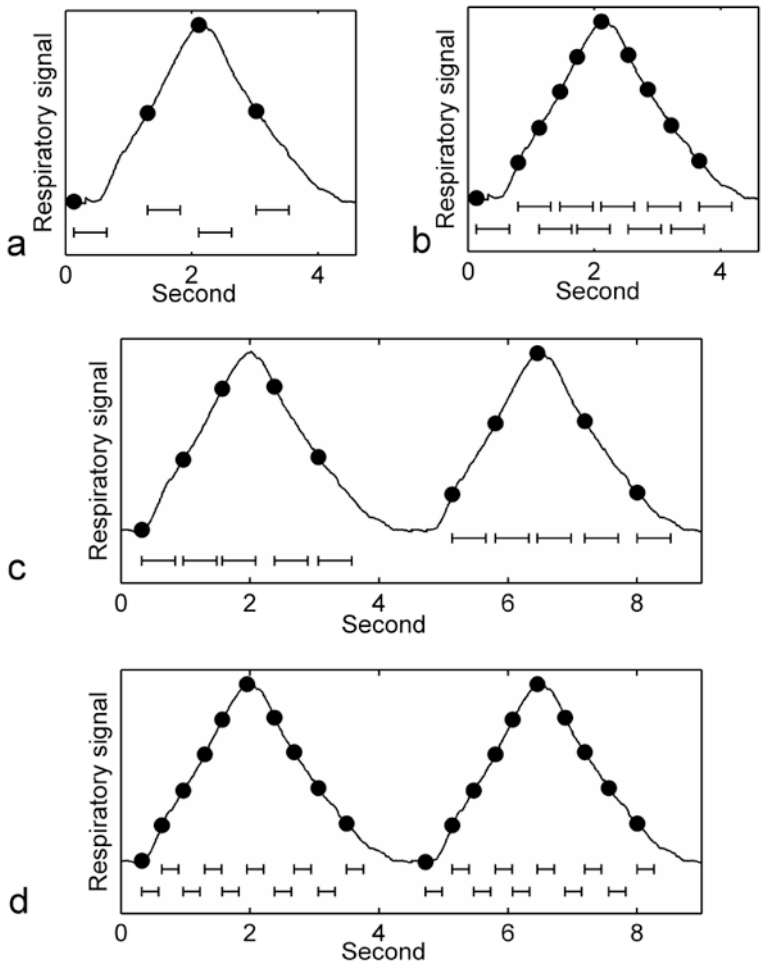

Figure 1.

(a) 4 respiratory states in a respiratory cycle, (b) 10 respiratory states in a respiratory cycle, (c) respiratory state splitting method and (d) multi-shot acquisition method to address the trigger missing issue. The dots indicate triggering respiratory amplitudes for individual respiratory states. The line bars under the curve indicate the required image acquisition times.

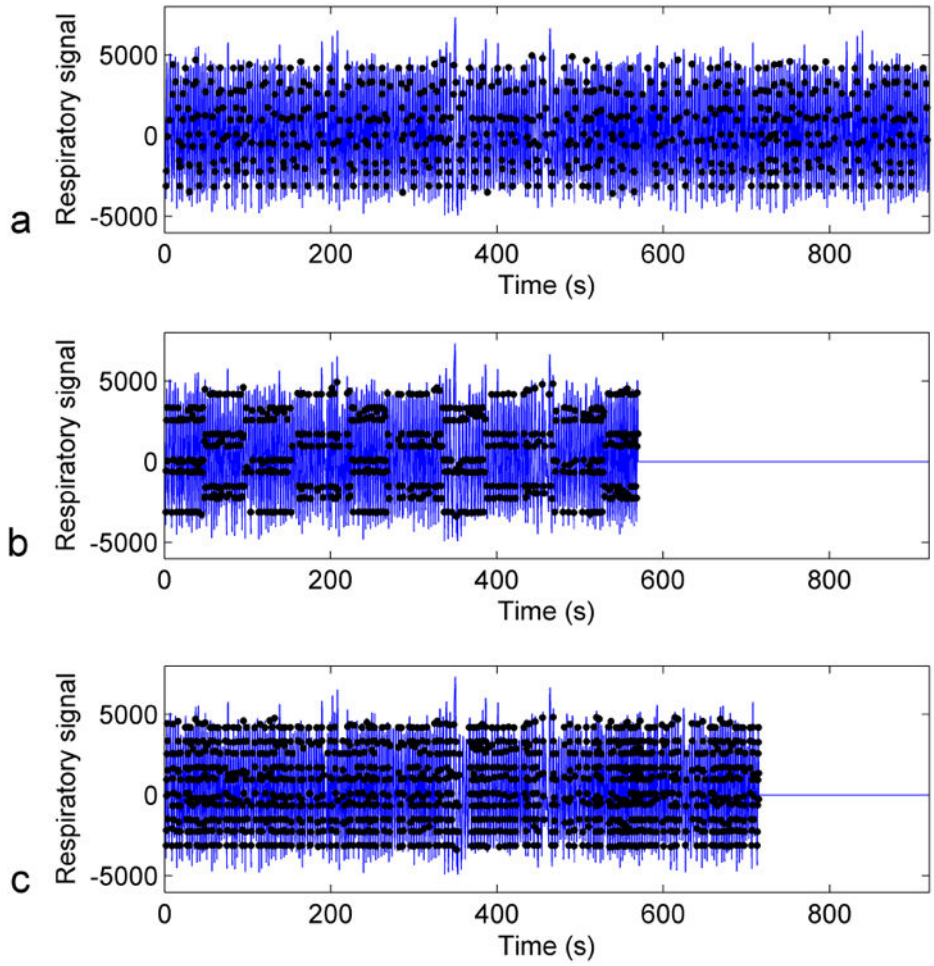

Figure 2.
Simulated 4DMRI acquisition using the prospective 4DMRI acquisition method incorporating (a) no intervention, (b) respiratory state splitting method and (c) multi-shot acquisition method.

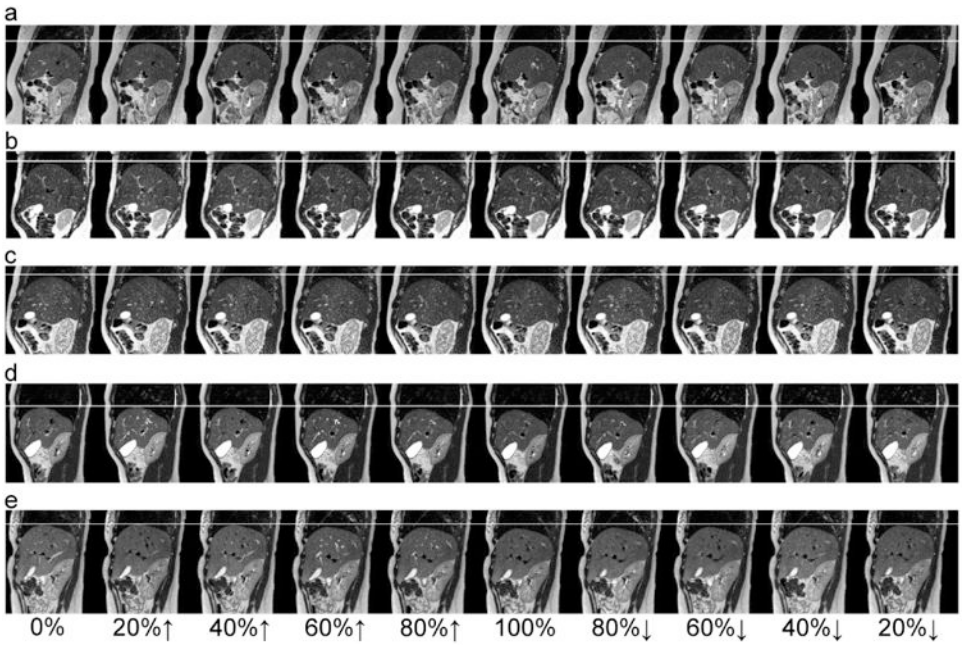

Figure 3.

Images of a representative sagittal slice at the 10 respiratory states (4DMRI with respiratory state splitting) for the 5 human subjects. The white line indicates the liver dome at the end of exhalation.

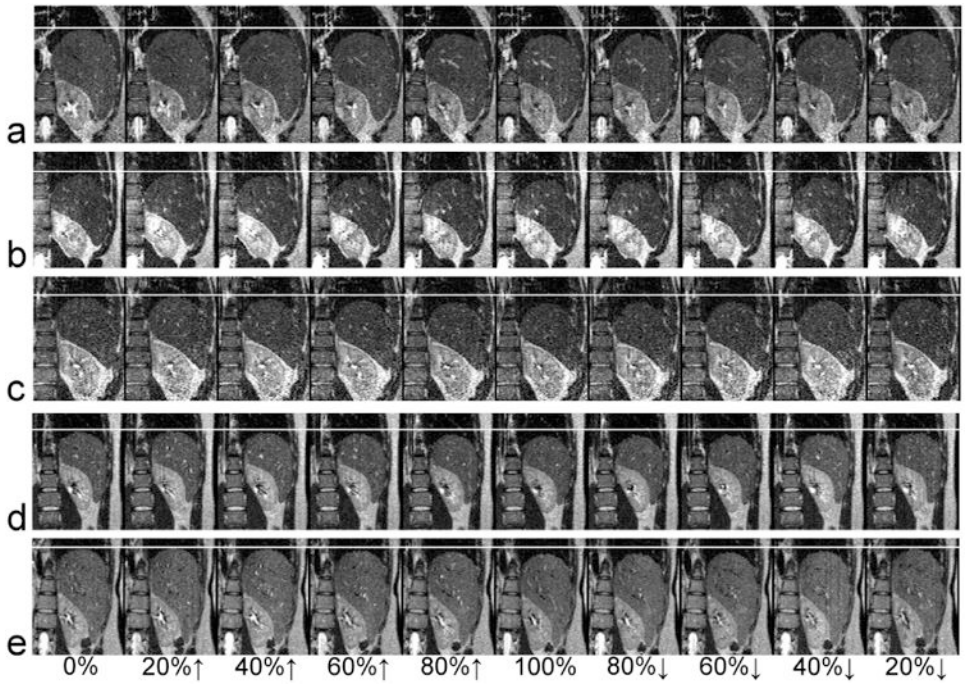

Figure 4.

Reconstructed images of a representative coronal plane at the 10 respiratory states (4DMRI with respiratory state splitting) for the 5 human subjects. The white line indicates the liver dome at the end of exhalation.

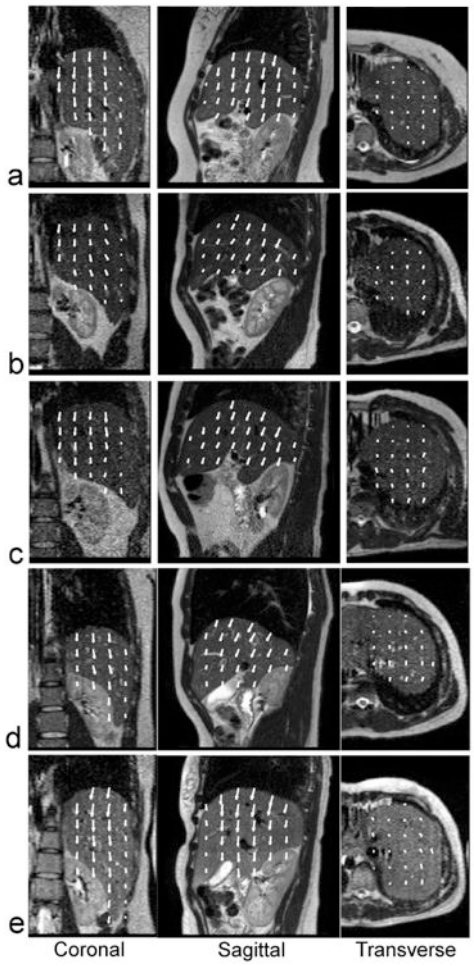

Figure 5.

Deformation vectors in liver on top of the end-of-exhalation images in three orthogonal views for the 5 human subjects. The arrows start from the locations at the end-of-exhalation and point towards the locations at the end-of-inhalation.

Table 1

Simulated acquisition time and percentage reduction in acquisition time for 4DMRI incorporating no intervention (None), respiratory state splitting (RSS) and multi-shot acquisition (MSA).

Subject	4DMRI_None (Min)	4DMRI_RSS (Min)	4DMRI_MSA (Min)	Acquisition time reduction (RSS)	Acquisition time reduction (MSA)
1	20.6	13.1	18.9	36%	8%
2	25.3	16.4	23.7	35%	6%
3	21.8	13.5	21.6	38%	1%
4	20.0	12.1	17.9	39%	9%
5	19.8	11.5	12.9	42%	35%
6	15.3	9.5	12.0	38%	22%
7	22.7	15.6	18.9	31%	17%
8	26.1	18.3	28.6	30%	-9%
9	19.8	13.1	19.1	34%	4%
10	14.7	8.9	13.1	39%	11%
Ave	20.6	13.2	18.7	36%	10%
p-value	---	4×10^{-9}	0.03	---	---